Biomaterials 335 (2026) 124388

Contents lists available at ScienceDirect

Biomaterials

journal homepage: www.elsevier.com/locate/biomaterials

Antifibrotic monocyte activation by nanoparticles resolves murine pulmonary fibrosis

Hannah Viola [a,b], Hannah Carter [b], Kate Griffin [a], Rita Medina Costa [b], Riley McDonald [a,d], Brennan Callow [d], Francina Gonzalez de Los Santos [b,c], Peyton Panovich [a], Sean Carey [a], Marisa Martinez [a], Ryan Chen [a], Zharia Hunter [a], Alexandra Piotrowski-Daspit [a,c], Gary Luker [a,d,e], Bethany B. Moore [b,c,*], Lonnie Shea [a,e,f,**]

[a] Department of Biomedical Engineering, University of Michigan, Ann Arbor, MI, 48109, USA
[b] Department of Microbiology and Immunology, University of Michigan, Ann Arbor, MI, 48109, USA
[c] Department of Internal Medicine - Division of Pulmonary and Critical Care Medicine, University of Michigan, Ann Arbor, MI, 48105, USA
[d] Department of Radiology, University of Michigan Medical School, Ann Arbor, MI, 48105, USA
[e] Biointerfaces Institute, University of Michigan, 48109, Ann Arbor, MI, 48109, USA
[f] Department of Chemical Engineering, University of Michigan, Ann Arbor, MI, 48109, USA

ARTICLE INFO

JEL classification:
Major-Biological sciences
Minor-Immunology and Inflammation

Keywords:
Immunoengineering
Nanoparticles
Immunomodulation
Fibrosis
Inflammation

ABSTRACT

Organ fibrosis presents a substantial disease burden with few therapeutic options. Innate immunity mediates fibrinogenesis, but also plays a major role in fibrinolysis. Here, we show that immunomodulatory nanoparticles (NPs) can harness this endogenous antifibrotic capacity by catalyzing monocyte activation leading to resolution of bleomycin-induced pulmonary fibrosis *in vivo*. Cargo-free NPs comprised of the degradable biopolymer poly (lactide-co-glycolide) (PLG) induce a transcriptional shift toward antifibrotic immune activation in profibrotic M2 macrophages (MΦs) *in vitro*. NPs stimulate M2 MΦs toward a glycolytic, rather than fatty acid oxidative, metabolism; suppress canonical M2 markers like arginase-1 (*Arg1*) and periostin ( ); and upregulate collagenases, hyaluronidases and immunoregulatory factors. When delivered intravenously *in vivo*, NPs resolve established bleomycin-induced pulmonary fibrosis and invert the trajectory of over 1000 genes from pre- to post-treatment according to bulk RNA-sequencing. NPs also suppress profibrotic signaling and increase expression of repair-associated pathways like peroxisome proliferator-activated receptor gamma (PPAR-γ), nuclear retinoic acid receptor (RAR), vascular endothelial growth factor (VEGF), and sphingolipid signaling in fibrotic lungs. Flow cytometry confirms that NPs induce monocyte recruitment to fibrotic lungs *via* enhanced integrin expression. Altogether, NPs induce a robust pro-regenerative signature comprised of ECM degradation, inflammation resolution, and tissue repair pathways, concomitant with increased NP+ monocyte recruitment to fibrotic lungs. This work demonstrates that monocytes are not intrinsically profibrotic, but rather, their effects are context-dependent, and they retain a capacity for fibrotic resolution under conditions that can be induced by materials with translational potential.

1. Introduction

Organ fibrosis is a common endpoint of chronic illness that contributes to the disease burden of 1 in 4 individuals worldwide [1], but has no cure and few therapeutic options. Fibrosis describes tissue scarring that occurs in the context of failed repair after severe or repetitive tissue injury or inflammation. Failed repair drives an inflammatory wound healing response that promotes the deposition of insoluble fibrillar collagens and other extracellular matrix (ECM) components by activated myofibroblasts. This ECM-rich microenvironment is itself profibrotic, perpetuating a cycle of dysregulated repair that ultimately compromises organ structure and function over time [2]. Small molecule inhibition of profibrotic signaling pathways with nintedanib and pirfenidone has slowed progression, but complete resolution remains

* Corresponding author. 1150 W. Medical Center Drive,MedSci II, Ann Arbor, MI, 48109, USA.
** Corresponding author. 1600 Huron Parkway, Ann Arbor, MI, 48109, USA.
E-mail addresses: bmoore@umich.edu (B.B. Moore), ldshea@umich.edu (L. Shea).

https://doi.org/10.1016/j.biomaterials.2026.124388
Received 24 April 2026; Accepted 15 June 2026
Available online 19 June 2026

elusive. The lack of success in treating fibrosis, despite decades of research, may relate, in part, to a limited focus on the promotion of antifibrotic responses. Fibrosis resolution is an active biological process that requires global structural reorganization that is accomplished by cooperation of all tissue cell types toward a homeostatic endpoint, but few therapeutic investigations have aimed to promote this process [2–4].

Mononuclear phagocytes (MPS) can be targeted to catalyze fibrosis resolution. MPS are central orchestrators of the tissue remodeling process, and as such they play a critical role in both the development and resolution of fibrosis [5]. Indeed, deletion of monocytes or MΦs prior to fibrotic emergence is protective [6], but their deletion during the spontaneous resolution phase delays resolution and exacerbates fibrosis [7,8]. These observations help explain why several large clinical trials have found little to no benefit for compounds that broadly inhibit inflammatory signaling, such as corticosteroids [9] and pentraxin-2 [10]. These compounds decrease profibrotic inflammation, but similarly prevent antifibrotic immune effector functions that require immune activation, such as tissue recruitment, differentiation, and secretion of inflammation-associated mediators [2,3,11], yielding little net benefit.

Here, we report that directed activation of myeloid cells with immunomodulatory polymeric NPs is sufficient to ameliorate established pulmonary fibrosis *in vivo* by inciting proresolving immune activation. Polymeric NPs profoundly alter the transcriptome of M2-polarized profibrotic MΦs *in vitro* by modulating their metabolism and signaling architecture to elicit an antifibrotic phenotype consisting of collagenases and immune-resolving mediators. Further, intravenous NPs target peripheral monocytes to induce their recruitment and activation in fibrotic lungs, leading to resolution of pulmonary fibrosis *in vivo*. Bulk RNA sequencing and flow cytometry of NP-treated lungs supports the notion that NPs drive an activated response from monocytes that accompanies fibrosis resolution *via* upregulation of ECM-degrading collagenases like matrix metalloproteinase 13 (MMP-13), collagen-binding phagocytic receptors like LAIR-1, and enzymes that produce immune-resolving lipids like prostaglandin E_2 (PGE_2). This work supports the emerging concept that innate immune activation is not universally pathological in the setting of fibrosis, but rather, the type and degree of inflammatory activation determines whether the response is protective or pathologic. These findings motivate renewed enthusiasm for immunomodulatory therapy as a fibrosis treatment, with the goal of harnessing endogenous antifibrotic immunity in a pro-resolving manner rather than broadly suppressing immunity.

2. Results

2.1. NPs polarize MΦs toward a proresolving phenotype in vitro

We first studied how NPs affect the phenotypic polarization of bone marrow-derived MΦs (BMDMs) *in vitro*. Although BMDM polarization states do not fully recapitulate *in vivo* effects [12], they can model the effect of NPs on well-characterized myeloid polarization states, which provides insight into their capacity for modulating phenotypes *in vivo*. Namely, we can evaluate how NPs affect BMDM polarization toward stereotypical M1 vs. M2 states that are linked to antifibrotic vs. profibrotic effects *in vivo*, respectively [13–15]. M2-like MΦs have been identified in fibrotic lungs and produce TGF-β, VEGF, arginase, and other profibrotic mediators, whereas M1-like MΦs or those with a "mixed" M1/M2 phenotype can be antifibrotic, producing collagenases, collagen receptors, and immune-resolving mediators [16,17]. These pro- and antifibrotic effects are related to the differences in the M1 vs. M2 states' metabolic, signaling, and epigenetic architectures. The M1 phenotype, induced by LPS and IFN-γ, utilizes aerobic glycolysis for energy and produces acute-phase response proteins like TNF-α, IL-1β, and reactive oxygen species (ROS) [18]. The M2 phenotype, induced by IL-4 and IL-13, utilizes fatty acid oxidation coupled to mitochondrial respiration for energy, is associated with arginase production and ornithine metabolism, and produces late-stage response mediators with roles in tissue repair, such as growth factors (TGF-β, VEGFs) and inflammation-controlling lipids and cytokines (e.g. specialized pro-resolving mediators, IL-10) [19]. Thus, we can correlate NPs' effects to these well-characterized states *in vitro* to determine whether NPs elicit profibrotic vs. antifibrotic phenotypes.

We first studied how NPs modify the phenotype of unpolarized (M0) MΦs toward M1 vs. M2 states. We fabricated polymeric NPs comprised of a poly(lactide-co-glycolide) (PLG) core coated with the surfactant poly(ethylene-alt-maleic anhydride) (PEMA) using oil-in-water emulsion followed by solvent evaporation as previously described [20] (Fig. 1A). NPs had a mean diameter of 609.22 ± 15.30 nm, polydispersity index (PDI) of 0.322 ± 0.099, and surface charge of −45.61 ± 5.48 mV across 5 independent batches (Fig. 1B, Fig. S1, Table S1). M0 BMDMs were cultured with 200 μg/mL NPs for 24 h, and their conditioned media was transferred into a myofibroblast scratch wound assay (Fig. 1C). qRT-PCR analysis of M0 MΦs showed that NPs downregulated the expression of M2 genes *Fizz1* and *Cd206* and upregulated M1 genes *iNos* and *Ccl3*/MIP-1α [21] (Fig. 1C *i*). Further, conditioned media from NP-treated BMDMs inhibited the migration of TGF-β-differentiated myofibroblasts in a scratch wound assay, indicating that NPs condition unpolarized BMDMs toward an antifibrotic phenotype that was more M1-like than vehicle-treated MΦs (Fig. 1C *iii*).

Next, we investigated the potential for NPs to shift the profibrotic phenotype of M2-polarized MΦs. BMDMs were polarized with IL-4 and IL-13 for 24 h (10 ng/μL each) and then treated with NPs for 24 h followed by next-generation bulk RNA sequencing (Illumina). NPs induced 6238 differentially expressed genes (DEGs) (3060 up, 3178 down, **File S1**), imparting a substantial transcriptional shift reflected by the robust separation between treatment groups on principal component analysis (Fig. 1D *i*) and hierarchical clustering of samples on a heatmap including all DEGs (Fig. 1D *ii*).

NP-induced DEGs reflect a shift in M2 MΦs toward a fibrosis-resolving phenotype with mixed M1 and M2 characteristics that comprises ECM-degrading enzymes and inflammation-resolving mediators (Table S2). NP-treated M2 MΦs upregulated ECM-degrading cathepsins, matrix metalloproteinases (MMPs), and hyaluronidases (e.g. *Ctsk*, *Mmp12*, *Hyal1)* [16,22], and the surface receptor *Mfge8* that binds collagen for phagocytotic clearance [23]. Concomitantly, NPs downregulated expression of ECM components including collagen, fibronectin, and chondroitin sulfate proteoglycan (e.g., *Col14a1*, *Fn1*, *Cspg5*). NPs also upregulated immunomodulatory receptors and ligands that have antifibrotic roles, such as the canonical aryl hydrocarbon receptor pathway [24], the enzyme *Ptges2* that produces prostaglandin E_2, and *Tollip*, a negative regulator of toll-like receptor (TLR) signaling whose dysfunction is one of only a few known genetic risk factors for developing pulmonary fibrosis [25–27]. Likewise, NPs downregulated profibrotic mediators including the growth factors TGF-β and periostin, numerous CCL- and CXCL-chemoattractants like *Ccl2* and *Ccl12*, and *C1q* complement components [28,29] (Table S2). NPs also reduced stereotypical M2-associated genes *Arg1*, *Retnla*/FIZZ-1, and *Cd163*. However, NPs also downregulated M1-associated genes, like *Il1b*, *Stat1*, and *Jak2*, suggesting that NPs do not unilaterally increase M1 phenotypic features as a consequence of decreasing M2 markers. However, a volcano plot shows that genes with the largest fold-change and lowest p-value are related to pro- or anti-fibrotic effects mediated by MΦs (Fig. 1D *iii*). Namely, NPs upregulate antagonists for profibrotic Wnt/β-catenin (*Sfrp5)* and IL-1 (*Il1rn*, *Npy*) [30–33]; inflammation controlling mediators (*Gpnmb* [34,35], *Cd200* [36], and *Dio2* [37,38]); and the HIF-1α-stabilizing factor *Igf2bp2* that promotes glycolytic metabolism [39,40]. In contrast, the volcano plot highlights the downregulation of *Mrc1*, a prototypical M2 marker gene [41]; *Il4i1*, which promotes M2 marker expression [42]; *Gda*, which promotes profibrotic IL-6 production [43]; and *C1qa*, which activates fibroblasts and is elevated in pulmonary fibrosis patients [28,29,44]. Taken together, these results suggest that NPs remodel MΦ phenotype from a profibrotic

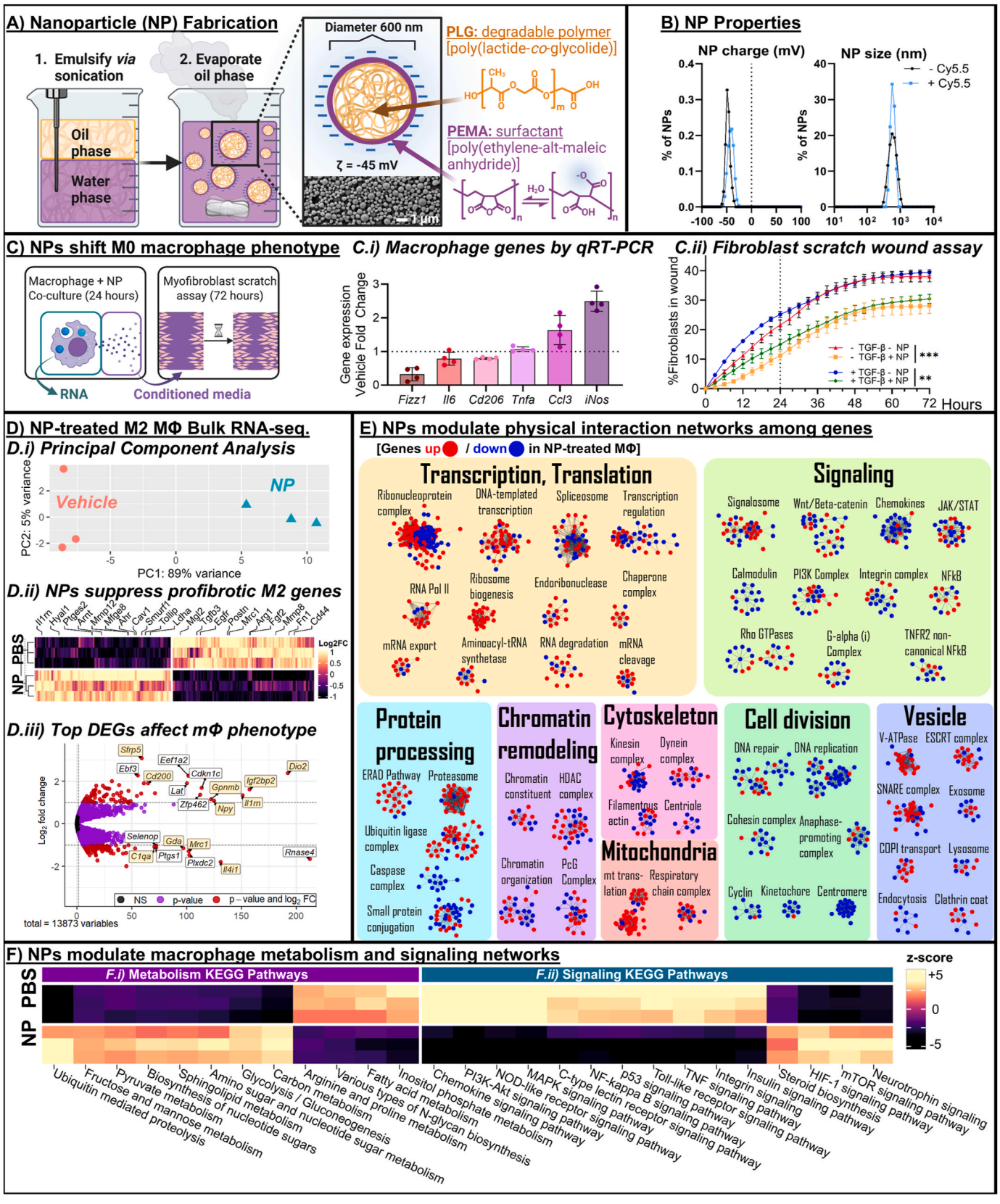

(caption on next page)

Fig. 1. NPs shift M2-polarized macrophages toward fibrosis resolution. **1A)** Nanoparticle fabrication process. Scale bar, 2 μm. **1B)** NP size and surface charge. **1C)** NPs were incubated with M0 BMDMs for 24 h followed by a myofibroblast scratch wound assay with BMDM conditioned media. **C.*i*** NPs inhibit M2-associated genes by qRT-PCR. **C.*ii*** BMDM conditioned media from NP-treated cells inhibits myofibroblast migration in a scratch wound assay. **1D)** NPs were incubated with M2-polarized BMDMs for 24 h followed by bulk RNA-sequencing. **D.*i*** PCA of all DEGs finds 89% of variation in first component, demonstrating that most gene expression variation is attributable to NP vs. vehicle conditions. **D.*ii*** Heatmap of all DEGs shows that over 6000 genes are robustly differentially expressed due to NPs, including upregulated antifibrotic macrophage genes and downregulated classically profibrotic M2 genes. **D.*iii*** Volcano plot of all DEGs emphasizes genes pertinent to macrophage phenotype that are both highly significant ($p \leq 0.05$) and ≥1 Log2 fold change in expression. **1E)** Protein-protein interaction network referencing the STRING physical interaction database shows that NPs modulate numerous important cellular functions. NPs upregulate endosome and protein-editing processes, and decrease cell division, signal transduction, and cytoskeletal components. **Statistics: C.*ii*** Two-way ANOVA with post-hoc Tukey's multiple comparisons test between all groups, $\alpha = 0.05$. *$p \leq 0.05$, **$p \leq 0.01$, ***$p \leq 0.001$, ****$p \leq 0.0001$. **1A, 1D.i)** Created with Biorender.com under applicable licensure. **Data points in C.*i* and D.*i* represent individual animals.**

M2 state to a matrix-degrading, inflammation-resolving state that does not clearly align with either M1 or M2 phenotypes.

Accompanying these changes, we observed remodeling of genes controlling transcriptional regulation. NPs upregulated the transcription factor (TF) peroxisome proliferator-activated receptor gamma (PPAR-γ), which is central to MΦs' roles in resolving inflammation, fibrosis, and wound repair [16,45–47], and shifted expression of TF lineages that orchestrate inflammatory responses and cell differentiation trajectories (i.e., Janus-associated kinase (JAK), JAGGED (JAG), signal transducer and activator of transcription (STAT), CCAAT/enhancer-binding proteins (CEBP), and interferon regulatory factors (IRF)) (Table S2). NP-treated MΦs also downregulated histone deacetylases, which have notably been a target of antifibrotic therapy [48], and increased expression of lysine demethylases (*Kdms*) and histone acetyltransferases (*Kats*), suggesting NPs stimulate remodeling of the epigenome. Finally, NPs increase DEAD box helicases that modify RNA transcription and metabolism to regulate innate immunity [49]. These changes reflect reworking of transcriptional architecture that accompanies substantial shifts in cellular function.

NPs also modified signaling architecture, especially tied to metabolism. We performed GSEA referencing the Kyoto Encyclopedia of Genes and Genomes (KEGG) to identify significantly enriched pathways in NP- vs. vehicle-treated M2 MΦs. NPs terms related to glycolysis, pyruvate metabolism, and nucleotide sugar metabolism and biosynthesis (Table S3, **File S2**), and downregulated pathways related to fatty acid oxidation, arginine/proline metabolism, and oxidative phosphorylation. These metabolic shifts are consistent with NP-mediated upregulation of M1-associated pathways, especially the concomitant upregulation of NFκB, HIF-1α, and mTOR cascades. NPs also downregulated M2-associated VEGF, MAPK, TLR, and PI3K/AKT cascades. However, NPs also upregulated the M2-promoting p53 pathway and downregulated M1-associated TNF signaling, showing that the polarization imparted by NPs is not unilaterally towards an M1-like phenotype. To further characterize changes in cellular architecture, we constructed a molecular interaction network between all DEGs referencing the STRING database of curated protein-protein binding relationships [50,51], identified non-interacting clusters of DEGs with similar functions based on gene set enrichment analysis (GSEA), and manually assigned clusters to major categories of cellular function. NPs suppressed genes related to cell division and signal transduction, and enhanced genes related to gene expression, protein editing, vesicle processing, and mitochondria (Fig. 1E). These changes reflect a shift in cellular activity away from cell division toward vesicle-mediated transport (e.g., SNARE complex, ESCRT complex, COPI transport), increased protein turnover (ribosome biogenesis, mRNA export, proteasome, ubiquitin ligase complex), and activation of mitochondria (mt translation).

Taken together, these findings show that the NPs substantially modulate transcriptional signatures of MΦ phenotype and effector functions by influencing metabolism, signaling, and epigenetic wiring. These changes promote a matrix-degrading, inflammation-resolving phenotype that accompanies an increase in M1-like features like glycolytic metabolism and a decrease in stereotypical M2 features like FIZZ-1, arginase, and fatty acid oxidative metabolism. However, NPs do not clearly induce an M1 phenotype, but rather produce a mixed phenotype. This is consistent with reports that antifibrotic macrophages adopt a mixed M1/M2 phenotype accompanied by ECM degrading enzymes and collagen binding receptors [16].

2.2. *Intravenous immunomodulatory NPs resolve in vivo pulmonary fibrosis at a late intervention stage*

We next investigated the capacity for NPs to exert antifibrotic effects on peripheral monocytes in bleomycin-induced pulmonary fibrosis. Peripheral monocytes recruit to fibrotic lungs and become fibrogenic M2-like monocyte-derived alveolar MΦs (moAMs) [14,52], and we found that NPs attenuate the profibrotic features of M2 MΦs and promote proresolving gene expression *in vitro*. Therefore, we hypothesized that NPs could similarly influence the activation of lung-recruited peripheral monocytes to attenuate their pathogenicity and possibly activate proresolving functions, such as the expression of ECM-degrading enzymes that we observed *in vitro*.

We aimed to capture translationally relevant therapeutic efficacy by intervening during active fibrotic remodeling rather than interfering with initial inflammation that establishes the fibrotic niche. Pulmonary fibrosis was induced using the oropharyngeal bleomycin mouse model as previously described (0.0125 U/mouse ~ 0.5 U/kg) [53]. The time-course of bleomycin-induced pulmonary fibrosis is well characterized, proceeding from initial inflammation during the first week, to fibroproliferation from ~7 to 21 days, followed by plateau and spontaneous regression from 21 to 56 days [54–57]. Thus, our intervention timepoint captures a stage wherein a fibrotic niche was established, but collagen deposition had not yet plateaued.

We first evaluated the biodistribution and clearance of NPs *in vivo*. NPs were fabricated with Cy5.5-labeled PLG for *in vivo* tracking, which did not appreciably affect NP size or surface charge (Fig. 1B). Solid organ biodistribution was evaluated 24 and 72 h after a single Cy5.5-NP dose delivered intravenously at our first dosing timepoint, Day 14 post-bleomycin. We confirmed *in vivo* degradation of NPs from the lungs, liver, spleen, and kidneys with half lives ranging from ~1 to 3 days (Fig. S2). We quantified the NPs' circulatory half life by serial sampling of peripheral blood, followed by automated image-based NP detection, as recently described [58]. NPs' half-life was 7.88 ± 3.35 min for a single dose in naive mice (Fig. S3), which falls within the range reported by others for NPs with similar size and surface charge [59,60].

The efficacy of intravenously delivered NPs at resolving active pulmonary fibrosis was evaluated using a single-dose bleomycin pulmonary fibrosis model (Fig. 2C) with dosing beginning after the establishment of a fibrotic lung microenvironment on Day 14 post-bleomycin. NPs were delivered intravenously *via* retro-orbital injection at 2 mg/dose in phosphate-buffered saline (Vehicle) beginning on day 14, followed by endpoint analysis on day 21 post-bleomycin (Fig. 2A). NPs reduced collagen deposition by Day 21 as quantified with whole lung hydroxyproline assay (Fig. 2B). Lungs trended towards improved lung ventilation and reduced ventilation heterogeneity on Day 29 post-bleomycin according to μCT imaging and ventilatory perfusion analysis (Fig. 1D) [61]. We also found that NPs do not affect clearance of *S. aureus in vivo* in fibrotic mice (Fig. S4).

Since NPs activate MPS *in vitro*, and monocyte activation can drive

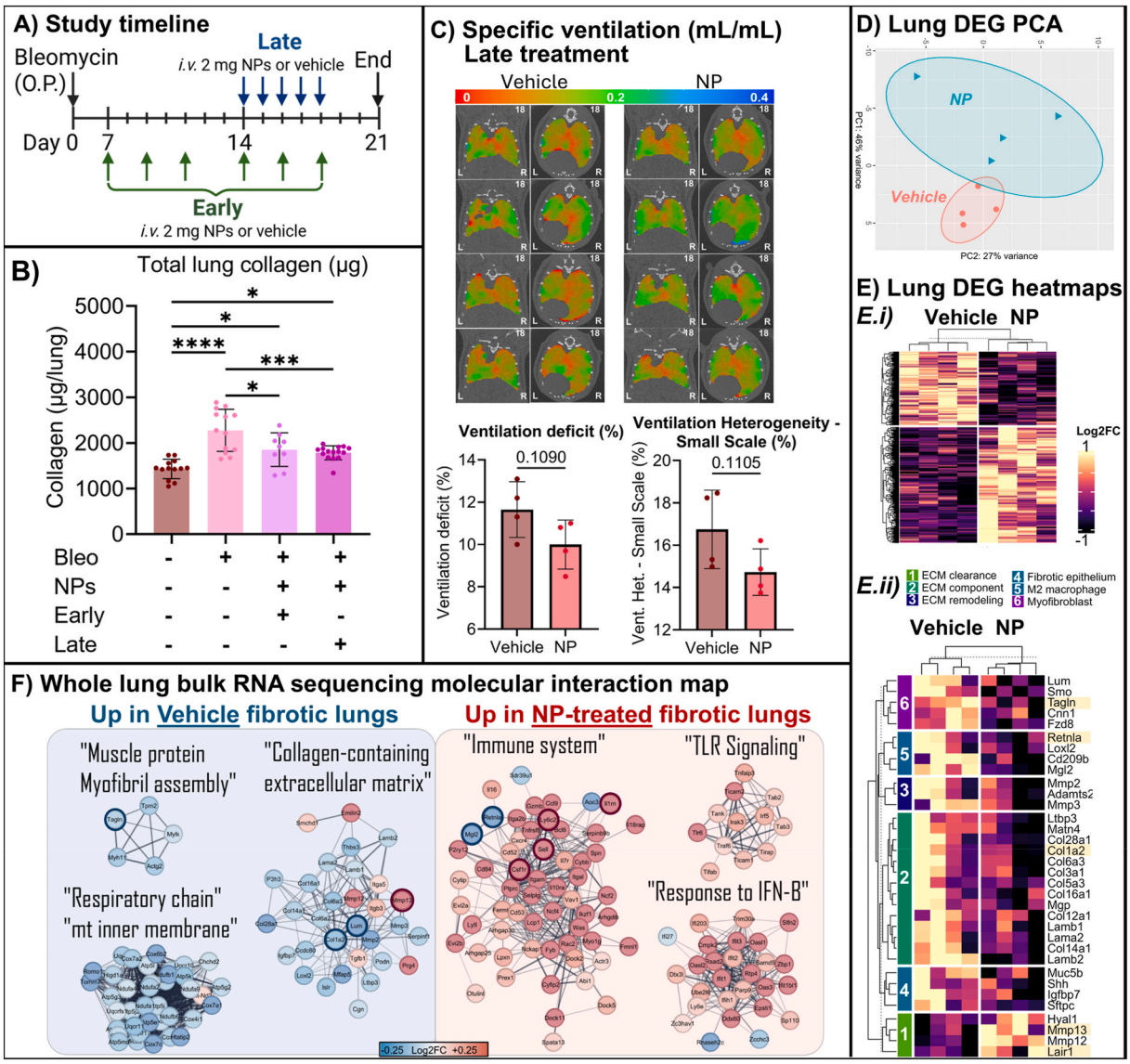

Fig. 2. NPs attenuate pulmonary fibrosis *in vivo* at a therapeutic timepoint and induce antifibrotic immune activation. 2A) Study timeline showing early vs. late delivery of NPs. 2B) Whole lung collagen measurement by hydroxyproline assay demonstrates that NPs at either timepoint ameliorate fibrosis. 2C) 4D µCT ventilation analysis demonstrates a trend toward improved ventilatory parameters in NP-treated animals. 2D) PCA Plot of all DEGs shows separation between NP- and Vehicle-treated lungs. Solid ovals, 80% confidence interval (CI); dotted ovals, 95% CI. 2E.*i)* Heatmap of all lung DEGs shows treatment group separation using unsupervised k-means clustering. Scale, −1 to 1 normalized Log2FoldChange. 2E.ii) Heatmap shows downregulation of fibrosis-associated genes (*Col1a2*, *Retnla*, *Tagln*) and upregulation of innate immune genes as well as immune-associated collagen-sensing (*Lair1*) and collagenase (*Mmp13*) genes. Scale, −1 to 1 normalized Log2-FoldChange. 2F) Whole lung bulk RNA-seq protein-protein interaction analysis finds downregulation of networks for collagen production program, muscle fiber machinery, and mitochondrial respiration, and upregulation of networks for innate immune activation. Statistics: B) One-way ANOVA with post-hoc Tukey's multiple comparisons test between all groups, $\alpha = 0.05$. *C)* Student's t-test, $\alpha = 0.05$. *$p \leq 0.05$, **$p \leq 0.01$, ***$p \leq 0.001$, ****$p \leq 0.0001$. 2A) Created with Biorender.com under applicable licensure. Data points in B) and D) represent individual animals.

establishment of the fibrotic niche, we asked whether NPs would exacerbate fibrogenesis. NPs' clinical translation would be impeded if NPs resolve a pre-existing fibrotic niche, but exacerbate its establishment by activating peripheral monocytes during fibrogenesis. We delivered NPs beginning during the peak recruitment of activated monocytes to the injured lungs, but prior to the emergence of appreciable fibrosis, on Day 7 post-bleomycin (early timepoint, Fig. 1A). Doses were spread across two weeks, instead of 5 consecutive days, to expose animals to NPs at timepoints spanning the evolution of the model from initial fibrogenesis on Day 7 to near-peak fibrosis on Day 21. If early NPs on Days 7-11 exacerbate fibrogenesis, or inhibit therapeutic effects of NPs delivered on Days 14-18, we would expect to see no decrease in collagen deposition between early NP- and vehicle-treated lungs by Day 21. Instead, early NPs similarly decrease collagen deposition when delivered with an early or late dosing scheme, suggesting that they do not activate monocytes in a way that enhances their contribution to fibrogenesis or inhibits therapeutic efficacy during fibroproliferation on Days 14-18.

Together these findings demonstrate that negatively charged, degradable polymeric NPs without therapeutic cargo can interrupt pulmonary fibrosis to reverse lung collagen deposition when administered systemically at a therapeutic timepoint without compromising host immunity.

2.3. Trajectory analysis reveals NP-driven resolving immune activation signature

We next assessed how NP delivery drove the pulmonary transcriptional landscape towards fibrosis resolution by conducting bulk RNA-sequencing on whole lung homogenates from 3 conditions: Day 14 (pre-treatment, n = 4), Day 21 NP (n = 4), and Day 21 Vehicle (n = 4) (mean 44 ± 7.7 million reads/sample). First, we compared NP- vs. Vehicle-treated lungs on day 21 and identified 1403 DEGs (862 up, 541 down, **File S3**) *via* Likelihood Ratio test in DESeq2 [62] with independent hypothesis weighting [63]. A PCA plot of these DEGs shows distinct transcription between groups (Fig. 2D), and unsupervised k-means clustering separates treatment groups on a heatmap of all DEGs (Fig. 2E *i*). A second heatmap (Fig. 2E *ii*) highlights the downregulation of genes associated with myofibroblasts, epithelial-mesenchymal transition, and M2 MΦs (Fig. 2D–Table S4) and shows that NPs increase transcripts for matrix-degrading enzymes like the collagenase *Mmp13* and collagen receptor *Lair1* (Fig. 2C–Table S4). To understand signaling networks in NP-treated lungs, we constructed a protein-protein interaction network referencing the STRING database and characterized

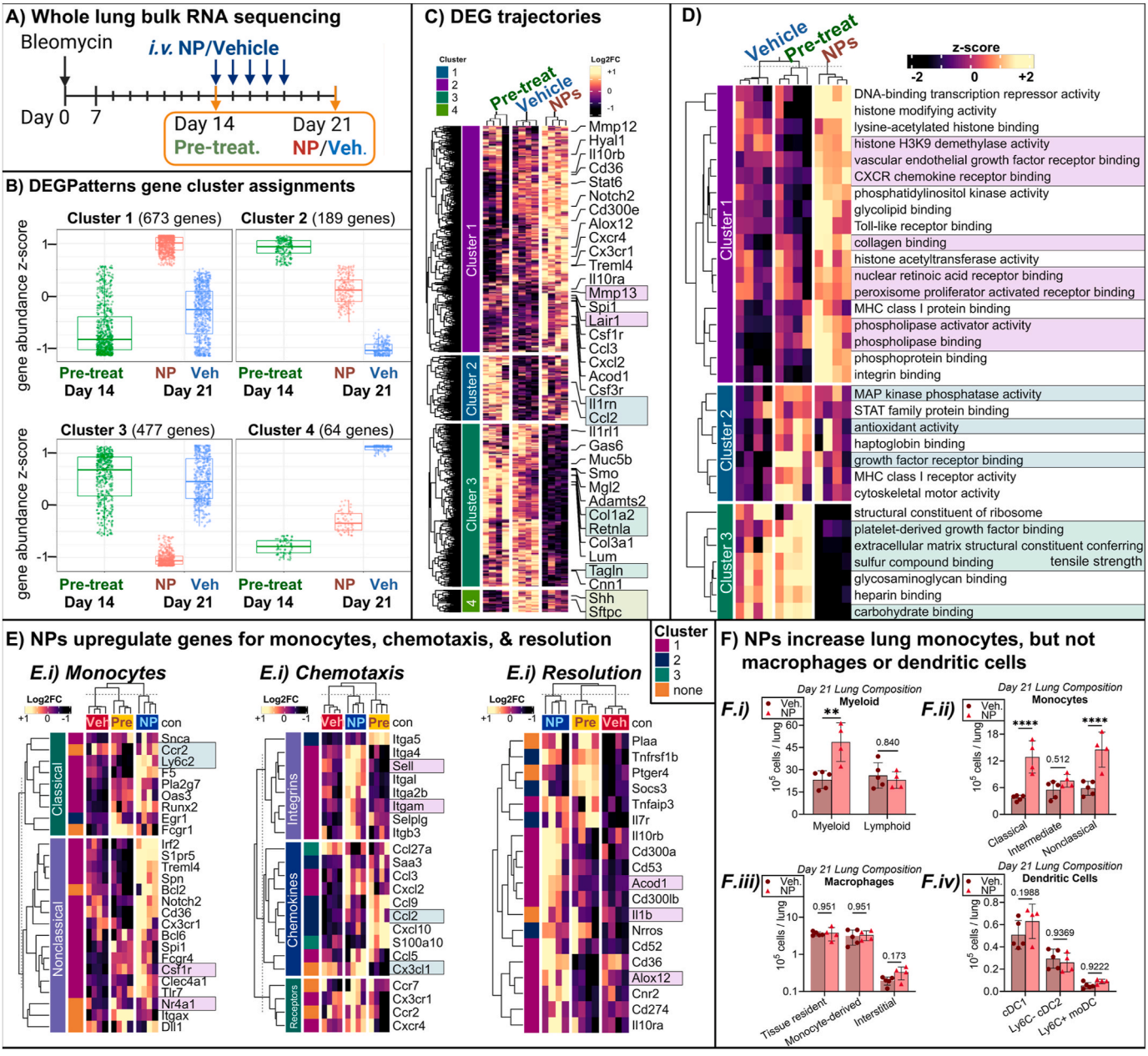

Fig. 3. NPs alter fibrotic trajectory towards inflammation resolution. 3A) Study timeline showing sequencing timepoints. 3B) DEG trajectory analysis shows that NPs change the trajectory of over 1000 genes in Clusters 1 and 3. 3C) DEG Heatmap with Day 14 demonstrates that the majority of genes with reversed trajectories concern immune-mediated fibrinolysis (cluster 1) and fibrosis (cluster 3). 3D) Heatmap of enriched pathways by trajectory cluster shows that NPs stimulate pro-resolving mediators like PPAR pathway, retinoic acid, and phospholipase activation in addition to collagen binding and epigenetic editing. NPs preserve early MAPK inhibition, antioxidant and regenerative responses, but suppress fibrotic ECM deposition and PDGF signaling. 3E) NP-treated lungs exhibited signatures for monocyte recruitment and antifibrotic resolving actions by myeloid cells. 3F) Flow cytometry confirmed that NP-treated lungs exhibit increased numbers of lung myeloid cells and monocytes, but not macrophages or dendritic cells. Statistics: *3F.i, iii, iv)* Two-way ANOVA with post-hoc Tukey's multiple comparisons test between conditions within each subset, $\alpha = 0.05$. *3F.iv)* Student's t-test, $\alpha = 0.05$. *p ≤ 0.05, **p ≤ 0.01, ***p ≤ 0.001, ****p ≤ 0.0001. 3A) Created with Biorender.com under applicable licensure. Data points in F) represent individual animals.

clusters using GSEA. This network showed that NPs downregulated transcriptional networks related to myofibrils, collagen-containing ECM, and mitochondrial respiration, and upregulated a large network of related immune signaling pathways (Fig. 2F). NPs also upregulated a TLR signaling network and a cluster of interferon (IFN) stimulated genes that GSEA labeled "response to IFN-β". Type I interferons, including IFN-β, have antifibrotic effects *in vivo* [64,65]. These data suggest that in murine lungs, NPs decreased profibrotic signaling and ECM deposition and increased ECM-degrading immunoregulatory pathways, similar to our findings *in vitro* in M2 polarized MΦs.

We next investigated the changes in NP-treated lungs pre-vs. post-treatment to understand how NPs alter the trajectory of gene expression in fibrotic lungs. Between NP and vehicle-treated lungs on Day 21, the majority of DEGs (60.4%) and enriched pathways (86.6%) were upregulated in NP-treated lungs, suggesting that NPs stimulate an active transcriptional response that reshapes the pulmonary environment, as opposed to passively inhibiting fibrogenic processes. Consensus clustering of day 21 DEGs was performed using the R package DEGReport [66] to characterize the trajectory of DEGs from day 14 to day 21 (Fig. 3A–C). Most DEGs induced by NPs represent a departure from the Day 14 profibrotic milieu. Clusters 1 and 3, which comprised the majority of DEGs, captured genes that were increased (673 genes) or decreased (477 genes) by NPs but remained relatively unchanged in vehicle-treated lungs from Day 14 to Day 21 (Fig. 3B and C). Clusters 2 (189 genes) and 4 (64 genes) captured genes preserved near Day 14 levels in NP-treated, but not vehicle, lungs. This analysis demonstrated that NPs primarily affect transcription by inducing novel gene expression programs that are absent in the untreated lungs at both timepoints, effectively pushing the lungs further away from pre-treatment conditions by either up- or down-regulating over 1000 genes that would otherwise maintain similar or lower expression by day 21.

Signaling networks in these trajectory clusters revealed that NPs activate a proresolving tissue remodeling process promoting tissue homeostasis. Genes in Cluster 1 included the leukocyte-specific collagen-binding receptor *Lair1* [67]; the collagenases *Mmp12* and *Mmp13*; hyaluronidase *Hyal1*; and leukocyte-specific gelatinase *Mmp25*/leukolysin [68]. Cluster 1 also contained inflammation-resolving mediators like *Alox12* [69], *Cybb/Nox2* [70], *Ccdc88a*/Girdin [71], and *Acod1/Irg1* [72,73] (Table S4). Enriched KEGG pathways for Cluster 1, upregulated in NP-treated but not vehicle or pre-treatment lungs, included collagen binding, retinoic acid receptor, phospholipase, peroxisome proliferator-activated receptor (PPAR), sphingolipid, and VEGF pathways (Fig. 3C–D, Table S5, **File S4**), consistent with lung injury resolution programs [74,75]. Other enriched pathways in Cluster 1 related to innate immune activation including leukocyte adhesion, recruitment, efferocytosis, and receptor-mediated phagocytosis (Table S5). Cluster 1 was also enriched in expression of innate immune sensors (NOD-like receptor, Toll-like receptors, C-type lectin receptors), and signaling cascades (JAK-STAT, NFκB) (Table S5). Cluster 2, preserved from Day 14 in NP- but not vehicle-treated lungs, included antioxidant activity, growth factor receptor binding, and TNF signaling. Cluster 3 (477 genes) was significantly downregulated from day 14 to day 21 in NP but not vehicle lungs and reflected pathological fibrotic processes. Enriched pathways were related to PDGF, ECM production, and sensing of ECM components like glycosaminoglycans, carbohydrates, heparin, and sulfur compounds (Fig. 3C–D, Table S5). Cluster 4 was only enriched for calmodulin binding GO pathways. Together with decreased total lung collagen and lower expression of fibrosis-associated genes, these transcriptional analyses are consistent with our *in vitro* findings that suggested NPs activate an antifibrotic innate immune activating response that rewires tissue-level function toward resolution of pulmonary fibrosis.

2.4. NPs stimulate lung recruitment of classical and nonclassical monocytes

Bulk RNA sequencing indicated antifibrotic innate immune activation reminiscent of our *in vitro* findings in M2 MΦ, which motivated studies on monocyte recruitment and activation in fibrotic lungs *in vivo*. We found that NPs induced a transcriptional signature for monocyte recruitment in fibrotic lungs, as well as signatures indicating elevated chemotaxis and secretion of proresolving mediators (Fig. 3E). Flow cytometry of lungs on Day 21 confirmed that total myeloid cell number in NP-treated lungs was increased (Gating strategy, Figs. S6 and S7). Among myeloid cells, classical and nonclassical monocytes (CMOs and NCMOs, respectively) were increased by NPs (Fig. 3Fi-*ii*), while the number of DCs, MΦs, and granulocytes were unchanged (Fig. 3F iii-iv, Fig. S5). Total lymphoid cell numbers were also unchanged by NPs (Fig. 3Fi). An increase in monocytes in NP-treated lungs is consistent with elevated expression of myeloid chemoattractants and integrins in NP- vs. vehicle-treated lung RNA sequencing data (Fig. 3E *i*). Taken together, NPs increase total lung monocyte recruitment to fibrotic lungs as profibrotic transcription decreases.

To identify whether monocytes were directly associated with NPs, we performed flow cytometry on lungs after treatment with fluorescently tagged NPs on day 14 (1 dose) or days 14-18 (5 NP doses) (Fig. 4A). We identified major myeloid subsets in the lung using established markers (Tables S7 and S8) [76–78]. The majority of recruited NP + lung cells on day 15 and day 21 were NCMOs, but not CMOs, followed by neutrophils and dendritic cells (Fig. 4B–C). NPs were sparsely found in MΦ subsets despite significantly increased monocyte numbers and high %NP+ in NCMOs (Fig. 4B–C), suggesting that NP + monocytes are unlikely to become profibrotic moAMs [52].

The surface expression by myeloid cells from NP-treated lungs was assessed to determine whether NPs directly influenced cell phenotypes upon reaching the lung. We analyzed neutrophils, NCMOs, interstitial monocytes (INTMOs), and monocyte-derived dendritic cells (moDCs), as these subsets had appreciable NP + cells in the lungs. Uniform manifold approximation and projection (UMAP) of $CD45^+$ myeloid cells revealed that NP + lung-recruited monocytes and neutrophils are phenotypically distinct from NP- cells in the same lungs (Gating, Fig. S8). The UMAP was constructed based on scaled, normalized mean fluorescence intensity (MFI) of all surface markers plus side scatter and forward scatter, excluding NP-Cy5.5 MFI. This analysis revealed that NP + lung recruited monocytes and neutrophils formed projections that extended to non-overlapping regions in the UMAP, showing that they deviate in MFI and/or scatter properties from NP- cells. Analysis of neutrophils, monocytes, and DCs from the circled regions of the UMAP (Fig. 4E) revealed that NP + monocytes and neutrophils ("NP+" on Fig. 4F legend) have greater side scatter and integrin expression than either NP- cells from the same lungs ("NP-") or vehicle treated lungs ("Veh") (Fig. 4F). CD11b + DCs that were NP + did not differ substantially from NP- or vehicle lungs, consistent with their greater overlap on UMAP with NP- DCs.

3. Discussion

Organ fibrosis is a prevalent endpoint of chronic illness worldwide and has few therapeutic options that delay, but do not resolve, progression of fibrosis. Tissue-recruited monocytes drive fibrogenesis, but inhibition of innate immune signaling with broad-spectrum immunomodulators like corticosteroids and pentraxin-2 did not ameliorate fibrosis in clinical trials. These findings suggest a critical role for monocytes in the resolution of fibrosis, which has since been demonstrated in multiple *in vivo* tissue fibrosis models [79]. Despite the importance of innate immune activation during fibrosis resolution, few studies have aimed to enhance this endogenous antifibrotic function as a therapeutic strategy.

We report that pharmacologic-free NPs comprised of the biomaterial

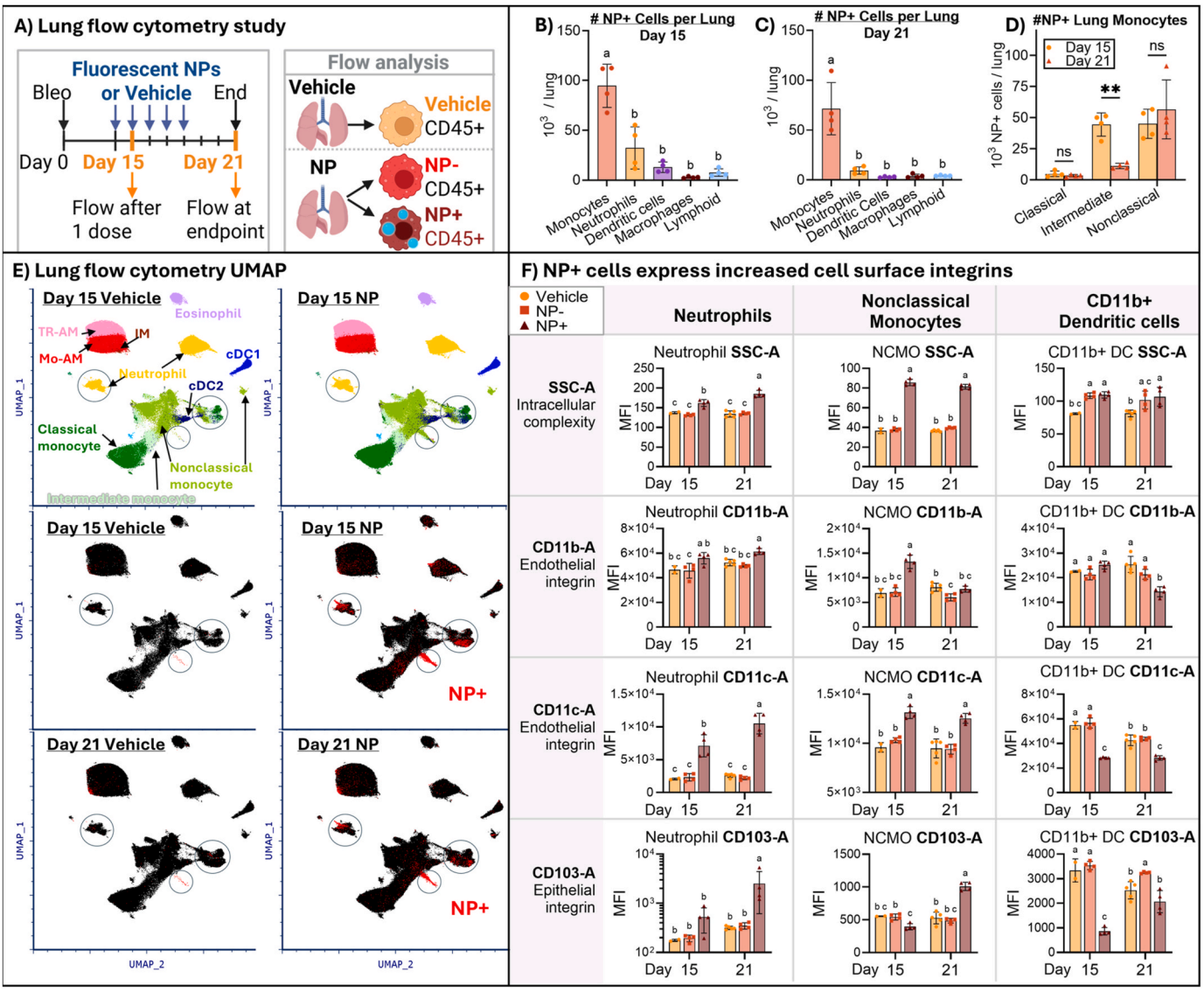

Fig. 4. NPs reside primarily in recruited monocytes. 4A) Study timeline showing flow cytometry timepoints. 4B, C) Composition of NP + lung cells on Day 15 (4B) and Day 21 (4C) shows that NPs are found mostly in lung-recruited monocytes. 4D) NP + lung monocytes are mostly intermediate or nonclassical. By Day 21, most NP + cells are NCMOs. 4E) UMAP of lung myeloid cells from flow cytometry data was constructed while excluding NP MFIs. UMAP segregates major cell types and identifies that NP + cells form phenotypically distinct projections in monocytes and neutrophils at both timepoints. 4F) Surface expression of integrins is upregulated by NP + lung myeloid cells (NP+), compared to both NP- cells in treated lungs (NP-), and all cells in untreated lungs (Vehicle). Statistics: 4B,C) One-way ANOVA with post-hoc Tukey's multiple comparisons test between all groups, $\alpha = 0.05$. 4D,F) Two-way ANOVA with post-hoc Tukey's multiple comparisons test between conditions, $\alpha = 0.05$. Letters represent statistically significant groups. *p ≤ 0.05, **p ≤ 0.01, ***p ≤ 0.001, ****p ≤ 0.0001. 4A) Created with Biorender.com under applicable licensure. Data points in B-D) and F) represent individual animals.

PLG have immunomodulatory effects that led to attenuated lung collagen deposition and a trend toward improved lung ventilation. Bulk RNA sequencing of NP-treated M2 MΦs showed that NPs reprogram metabolism, signaling networks, and epigenetics to favor an ECM-degrading, inflammation resolving phenotype with suppressed M2 MΦ markers (Fig. 1). *In vivo*, lung bulk RNA sequencing showed that NPs recapitulate their *in vitro* effects by reducing M2 MΦ markers, ECM expression, and fatty acid oxidative metabolism while increasing pro-resolving immunity and ECM-degrading enzymes, leading to reduced total lung collagen on Day 21 (Fig. 2). Transcriptional comparison of lungs from pre-to post-treatment showed that NPs uniquely stimulate this innate immune response rather than preserving existing antifibrotic responses (Fig. 3). Finally, flow cytometry found that total lung monocyte numbers are increased in NP-treated animals, and most NP + lung cells are NCMOs. MFI analysis found that NP + myeloid cells increase expression of the integrins CD11b, CD11c, and CD103 (Fig. 4), consistent with increased tissue recruitment. Taken together, we conclude that NP treatment after the establishment of pulmonary fibrosis on day 14 post-bleomycin induces peripheral monocyte activation and recruitment into fibrotic lungs to mediate resolution of the fibrotic milieu and a reduction in total lung collagen.

We found that NPs double the number of CMOs in fibrotic lungs while exerting antifibrotic effects (Fig. 3F). This result is unexpected based on prior findings that CMOs and their derivative moAMs drive fibrogenesis, and ablation of either of these populations prevents fibrosis [52,80]. Our results could be explained by the fact that, despite increased CMOs, NP-treated lungs did not have increased moAMs or moDCs. Instead, NP-treated lungs had twice as many NCMOs, which also derive from CMOs, and are considered inflammation-resolving and tissue regenerative [81,82]. In liver and lung fibrosis, Ly6C^{lo} monocytes/macrophages similar to NCMOs have been identified as mediators of spontaneous resolution [83–85]. Therefore, the NP-mediated increase

in total lung NCMOs could contribute to NPs' effects in mediating fibrinolysis.

We showed that NPs bias MPS toward an ECM-degrading, immunoregulatory state in both M2 MΦs *in vitro* and lung-recruited NCMOs *in vivo*, and stimulated M0 MΦs to inhibit fibroblast migration, despite appreciable biological differences between these cell states. Therefore, NPs' effects appear relatively independent of the initial MPS state, suggesting that NPs stimulate a strong, specific response program that triggers antifibrotic and immunoregulatory effects. Such a broad effect is likely the result of activating conserved cellular pathways, such as a characteristic response to phagocytosis. For example, we found that NPs upregulate the pleiotropic immunoregulatory transcription factor PPAR-γ, a master regulator of proresolving activation in monocytes [86] that can be triggered by efferocytosis [23,47]. Others have found that post-phagocytic 'satiated' MΦs have fibrinolytic properties [87,88]. NPs have comparable size and surface charge as apoptotic bodies, suggesting that NPs could trigger efferocytosis-like programming in MPS. This would be consistent with increased expression of ECM degradation and inflammation-resolving patterns that we observed across multiple MPS *in vitro* and *in vivo*. We have previously shown that NPs with similar composition and physical properties activate splenic phagocytes in naïve C57BL/6J mice [89], suggesting that NPs exert phenotypic reprogramming independent of inflammatory context.

Other molecular mechanisms underpinning the effects of cargo-less NPs remain under investigation. NPs acquire a protein corona from serum proteins that was recently shown to affect their inflammation-modulating properties imparted to the phagocytosing cells [90]. Internalization of particles in our size range (~600 nm) proceeds *via* receptor-mediated phagocytosis, which can trigger signaling cascades that remodel phagocyte functions [91]. Within the phagolysosome, NP degradation produces lactic acid, which can modulate monocyte metabolism [92,93], and altered monocyte phenotypes near lactate-producing biomaterials *in vivo* [94].

Our results challenge the notion that monocytes are unilaterally pathogenic in pulmonary fibrosis. Although monocyte recruitment and effector functions mediate fibrogenesis and associate with acute exacerbations [95,96], this does not preclude a beneficial role during fibrinolytic remodeling. Rather, monocytes participate centrally in both fibrogenesis and fibrinolysis due to their ability to interact directly with the extracellular matrix and structural cells that are involved in both processes [84]. This dual role may explain why attempts to suppress monocyte responses have not yielded therapeutic benefit. Effective therapies would therefore harness beneficial monocyte responses while suppressing pathogenic activation. However, manipulation of peripheral monocytes presents risks. Adverse monocyte activation in the systemic circulation can lead to deadly complications including cytokine storm [97], disseminated intravascular coagulation [98], and indirect acute lung injury [99]. In pulmonary fibrosis patients, systemic monocyte activity is associated with acute exacerbation and disease progression [96]. Adverse events such as those mentioned here were not observed for the NPs delivered in this study.

The limitations of the study are determined largely by our choice of animal model. We used a single-dose bleomycin lung injury to young male mice. Male mice were employed because ~70% of pulmonary fibrosis patients are male [100], but follow-up is needed to evaluate sex differences in efficacy. Young mice (6-8 weeks) were used due to logistic limitations, but aged mice (>72 weeks) would more accurately capture the biology relevant to human pulmonary fibrosis as most patients present above age 60[57]. Single-dose bleomycin in young mice is spontaneously self-limiting, but is non-resolving in aged mice, underscoring the importance of capturing senescence in models of progressive lung fibrosis [101]. Other *in vivo* lung fibrosis models could be evaluated such as overexpression of TGF-β or *Sftpc* to validate the NP efficacy. Additionally, we did not evaluate human cells in this study, which could improve our ability to predict NP effects in human fibrosis patients prior to clinical application.

In summary, we showed that NPs comprised of degradable biomaterials can activate monocytes to resolve established pulmonary fibrosis *in vivo*. Therapeutic promotion of endogenous antifibrotic immunity holds potential to complement antifibrotic therapy to facilitate wholistic resolution of pulmonary fibrosis. The NPs are comprised of PLG, an FDA-approved biomaterial that has already been used in human NP-based therapies. The profound immunomodulatory effects described here underscores the opportunity for cargo-free PLG NPs to be a safe and effective regenerative therapeutic for tissue fibrosis.

Significance statement

Organ fibrosis can follow from tissue injury and substantially impairs organ function, but it is incurable and has limited therapeutic options. Myeloid immune cells drive fibrosis onset and progression, but they can also mediate fibrosis resolution. We used polymeric NPs made from clinically translatable biomaterials to harness the antifibrotic capacity of immune cells as a fibrosis therapy. We found that intravenous NPs can reprogram myeloid cells to acquire an antifibrotic phenotype in a mouse model of pulmonary fibrosis. NPs increased myeloid activation and pulmonary recruitment while decreasing fibrosis, showing that directed immune activation, instead of suppression, could be an effective therapeutic strategy for fibrosis.

CRediT authorship contribution statement

Hannah Viola: Conceptualization, Data curation, Formal analysis, Investigation, Methodology, Project administration, Software, Validation, Visualization, Writing – original draft, Writing – review & editing. **Hannah Carter:** Investigation, Methodology, Writing – review & editing. **Kate Griffin:** Investigation, Writing – review & editing. **Rita Medina Costa:** Formal analysis, Investigation, Writing – review & editing. **Riley McDonald:** Formal analysis, Investigation, Writing – review & editing. **Brennan Callow:** Investigation, Writing – review & editing. **Francina Gonzalez de Los Santos:** Investigation, Methodology, Writing – review & editing. **Peyton Panovich:** Investigation, Methodology, Writing – review & editing. **Sean Carey:** Investigation, Methodology, Writing – review & editing. **Marisa Martinez:** Investigation, Writing – review & editing. **Ryan Chen:** Investigation, Writing – review & editing. **Zharia Hunter:** Investigation, Writing – review & editing. **Alexandra Piotrowski-Daspit:** Resources, Supervision, Writing – review & editing. **Gary Luker:** Resources, Supervision, Writing – review & editing. **Bethany B. Moore:** Conceptualization, Funding acquisition, Methodology, Resources, Supervision, Writing – review & editing. **Lonnie Shea:** Conceptualization, Funding acquisition, Methodology, Resources, Supervision, Writing – review & editing.

Declaration of competing interest

The authors declare the following financial interests/personal relationships which may be considered as potential competing interests: Lonnie Shea, Bethany Moore report financial support provided by National Institutes of Health. Lonnie Shea reports a relationship with Cour Pharmaceuticals Development Co Inc that includes: consulting or advisory, equity or stocks, and funding grants. Lonnie Shea has patent #US20150190485A1 licensed to Cour Pharmaceuticals. Other authors0declare that they have no known competing financial interests or personal relationships that could have appeared to influence the work reported in this paper.

Acknowledgements

Bulk RNA library preparation and next-generation sequencing were carried out by the Advanced Genomics Core at the University of Michigan. Flow cytometry data were collected within the University of Michigan's Flow Cytometry Core Facility. Electron microscopy was

conducted at the University of Michigan Center for Materials Characterization. Figures were created with BioRender.com under applicable licensing agreements SB29UX9NMY, ZV29UX9VG0, NX29UX9X81, PK29UX9Z4R, SE29UX9HB6. The authors acknowledge funding from The University of Michigan Multidisciplinary Training in Lung Disease (5T32HL007749-33) to HV, R35HL176572 to BBM, and R01EB036030 and R01AI148076 to LS.

Appendix A. Supplementary data

Supplementary data to this article can be found online at https://doi.org/10.1016/j.biomaterials.2026.124388.

Data availability

Count matrices, code, and code outputs for both bulk RNA sequencing datasets is available at: https://github.com/shea-lab/Viola_2026_NP.Fibrosis. All other data available upon reasonable request to the authors. Raw sequencing data are available on Gene Expression Omnibus GSE336548 and GSE336549. .

References

[1] X. Zhao, J.Y.Y. Kwan, K. Yip, P.P. Liu, F.-F. Liu, Targeting metabolic dysregulation for fibrosis therapy, Nat. Rev. Drug Discov. 19 (2020) 57–75.
[2] S.M. Fortier, E.F. Redente, M. Peters-Golden, Reimagining fibrosis research, outcomes, and therapeutics through the lens of resolution, Semin. Respir. Crit. Care Med. (2025), https://doi.org/10.1055/a-2666-7479, 10.1055/a-2666-7479.
[3] J.-I. Jun, L.F. Lau, Resolution of organ fibrosis, J. Clin. Investig. 128 (2018) 97–107.
[4] K. Atabai, C.D. Yang, M.J. Podolsky, You say you want a resolution (of fibrosis), Am. J. Respir. Cell Mol. Biol. 63 (2020) 424–435.
[5] S.W. Glasser, et al., Mechanisms of lung fibrosis resolution, Am. J. Pathol. 186 (2016) 1066–1077.
[6] B.B. Moore, et al., CCR2-Mediated recruitment of fibrocytes to the alveolar space after fibrotic injury, Am. J. Pathol. 166 (2005) 675–684.
[7] M.A. Gibbons, et al., Ly6Chi monocytes direct alternatively activated profibrotic macrophage regulation of lung fibrosis, Am. J. Respir. Crit. Care Med. 184 (2011) 569–581.
[8] J.S. Duffield, et al., Selective depletion of macrophages reveals distinct, opposing roles during liver injury and repair, J. Clin. Investig. 115 (2005) 56–65.
[9] T. Pitre, et al., Systemic corticosteroids in fibrotic lung disease: a systematic review and meta-analysis, BMJ Open Respir. Res. 10 (2023).
[10] L. Richeldi, et al., Zinpentraxin alfa for idiopathic pulmonary fibrosis: the randomized phase III STARSCAPE trial, Am. J. Respir. Crit. Care Med. 209 (2024) 1132–1140.
[11] Y. Koda, N. Nakamoto, T. Kanai, Regulation of progression and resolution of liver fibrosis by immune cells, Semin. Liver Dis. 42 (2022) 475–488.
[12] M. Nahrendorf, F.K. Swirski, Abandoning M1/M2 for a network model of macrophage function, Circ. Res. 119 (2016) 414–417.
[13] T. Rőszer, Understanding the mysterious M2 macrophage through activation markers and effector mechanisms, Mediat. Inflamm. 2015 (2015) 816460.
[14] T.T. Braga, J.S.H. Agudelo, N.O.S. Camara, Macrophages during the fibrotic process: M2 as friend and foe, Front. Immunol. 6 (2015).
[15] R. Zhang, et al., Favipiravir ameliorates bleomycin-induced pulmonary fibrosis by reprogramming M1/M2 macrophage polarization, Int. Immunopharmacol. 131 (2024) 111774.
[16] A. Adhyatmika, K.S.S. Putri, L. Beljaars, B.N. Melgert, The elusive antifibrotic macrophage, Front. Med. 2 (2015).
[17] S. Chen, et al., Modulation of anti-cardiac fibrosis immune responses by changing M2 macrophages into M1 macrophages, Mol. Med. 30 (2024) 88.
[18] S. Galván-Peña, L.A.J. O'Neill, Metabolic reprograming in macrophage polarization, Front. Immunol. 5 (2014).
[19] D. Zhou, et al., Macrophage polarization and function: new prospects for fibrotic disease, Immunol. Cell Biol. 95 (2017) 864–869.
[20] H. Jeffery, S.S. Davis, D.T. O'Hagan, The preparation and characterisation of poly (lactide-co-glycolide) microparticles. I: Oil-in-water emulsion solvent evaporation, Int. J. Pharm. 77 (1991) 169–175.
[21] Z. He, et al., The interaction between different types of activated RAW 264.7 cells and macrophage inflammatory protein-1 alpha, Radiat. Oncol. 6 (2011) 86.
[22] S. Taddese, et al., MMP-12 catalytic domain recognizes and cleaves at multiple sites in human skin collagen type I and type III, Biochim. Biophys. Acta BBA - Proteins Proteomics 1804 (2010) 731–739.
[23] K. Atabai, et al., Mfge8 diminishes the severity of tissue fibrosis in mice by binding and targeting collagen for uptake by macrophages, J. Clin. Investig. 119 (2009) 3713–3722.
[24] Carter, H. et al. CD103+ dendritic cell–fibroblast crosstalk via TLR9, TDO2, and AHR signaling drives lung fibrogenesis. JCI Insight 10, e177072.
[25] X. Liu, et al., Tollip orchestrates macrophage polarization to alleviate intestinal mucosal inflammation, J. Crohns Colitis 16 (2022) 1151–1167.
[26] S. Venkatasubramanian, et al., TOLLIP inhibits lipid accumulation and the integrated stress response in alveolar macrophages to control Mycobacterium tuberculosis infection, Nat. Microbiol. 9 (2024) 949–963.
[27] J.H. Lipinski, et al., Toll-interacting protein and altered lung microbiota in idiopathic pulmonary fibrosis, Am. J. Respir. Crit. Care Med. 206 (2022) 224–227.
[28] W. Kou, et al., High complement protein C1q levels in pulmonary fibrosis and non-small cell lung cancer associated with poor prognosis, BMC Cancer 22 (2022) 110.
[29] T. Ogawa, S. Shichino, S. Ueha, S. Ogawa, K. Matsushima, Complement protein C1q activates lung fibroblasts and exacerbates silica-induced pulmonary fibrosis in mice, Biochem. Biophys. Res. Commun. 603 (2022) 88–93.
[30] T. Trinh-Minh, et al., Noncanonical WNT5A controls the activation of latent TGF-β to drive fibroblast activation and tissue fibrosis, J. Clin. Investig. 134 (2024).
[31] P.F. Piguet, C. Vesin, G.E. Grau, R.C. Thompson, Interleukin 1 receptor antagonist (IL-1ra) prevents or cures pulmonary fibrosis elicited in mice by bleomycin or silica, Cytokine 5 (1993) 57–61.
[32] N. Chatani, et al., Secreted frizzled-related protein 5 (Sfrp5) decreases hepatic stellate cell activation and liver fibrosis, Liver Int. 35 (2015) 2017–2026.
[33] J. Itano, et al., Neuropeptide Y antagonizes development of pulmonary fibrosis through IL-1β inhibition, Am. J. Respir. Cell Mol. Biol. 67 (2022) 654–665.
[34] K. Kumagai, et al., Glycoprotein nonmetastatic Melanoma B (Gpnmb)-Positive macrophages contribute to the balance between fibrosis and fibrolysis during the repair of acute liver injury in mice, PLoS One 10 (2015) e0143413.
[35] King, E. M. et al. Gpnmb and Spp1 mark a conserved macrophage injury response masking fibrosis-specific programming in the lung. JCI Insight 9, e182700.
[36] R.J. Snelgrove, et al., A critical function for CD200 in lung immune homeostasis and the severity of influenza infection, Nat. Immunol. 9 (2008) 1074–1083.
[37] S.-F. Ma, et al., Type 2 deiodinase and host responses of sepsis and acute lung injury, Am. J. Respir. Cell Mol. Biol. 45 (2011) 1203–1211.
[38] J. Kwakkel, et al., A novel role for the thyroid hormone-activating enzyme type 2 deiodinase in the inflammatory response of macrophages, Endocrinology 155 (2014) 2725–2734.
[39] Y. Zhou, et al., The m6A reader IGF2BP2 regulates glycolytic metabolism and mediates histone lactylation to enhance hepatic stellate cell activation and liver fibrosis, Cell Death Dis. 15 (2024) 189.
[40] X. Wang, et al., The m6A reader IGF2BP2 regulates macrophage phenotypic activation and inflammatory diseases by stabilizing TSC1 and PPARγ, Adv. Sci. 8 (2021) 2100209.
[41] L. He, et al., Global characterization of macrophage polarization mechanisms and identification of M2-type polarization inhibitors, Cell Rep. 37 (2021).
[42] Y. Yue, et al., IL4I1 is a novel regulator of M2 macrophage polarization that can inhibit T cell activation via L-Tryptophan and arginine depletion and IL-10 production, PLoS One 10 (2015) e0142979.
[43] C.-L. Lee, et al., Glycodelin-A stimulates Interleukin-6 secretion by human monocytes and macrophages through L-selectin and the extracellular signal-regulated kinase pathway, J. Biol. Chem. 287 (2012) 36999–37009.
[44] T. Ogawa, S. Shichino, S. Ueha, K. Bando, K. Matsushima, Profibrotic properties of C1q+ interstitial macrophages in silica-induced pulmonary fibrosis in mice, Biochem. Biophys. Res. Commun. 599 (2022) 113–119.
[45] K. Asada, S. Sasaki, T. Suda, K. Chida, H. Nakamura, Antiinflammatory roles of peroxisome proliferator–activated receptor γ in human alveolar macrophages, Am. J. Respir. Crit. Care Med. 169 (2004) 195–200.
[46] H. Chen, et al., Macrophage peroxisome proliferator-activated receptor γ deficiency delays skin wound healing through impairing apoptotic cell clearance in mice, Cell Death Dis. 6 (2015) e1597–e1597.
[47] Y.-S. Yoon, et al., PPARγ activation following apoptotic cell instillation promotes resolution of lung inflammation and fibrosis via regulation of efferocytosis and proresolving cytokines, Mucosal Immunol. 8 (2015) 1031–1046.
[48] X. Lyu, M. Hu, J. Peng, X. Zhang, Y.Y. Sanders, HDAC inhibitors as antifibrotic drugs in cardiac and pulmonary fibrosis, Ther. Adv. Chronic Dis. 10 (2019) 2040622319862697.
[49] O. Andrisani, et al., Biological functions of DEAD/DEAH-box RNA helicases in health and disease, Nat. Immunol. 23 (2022) 354–357.
[50] N.T. Doncheva, et al., Cytoscape stringApp 2.0: analysis and visualization of heterogeneous biological networks, J. Proteome Res. 22 (2023) 637–646.
[51] D. Szklarczyk, et al., The STRING database in 2025: protein networks with directionality of regulation, Nucleic Acids Res. 53 (2025) D730–D737.
[52] A.V. Misharin, et al., Monocyte-derived alveolar macrophages drive lung fibrosis and persist in the lung over the life span, J. Exp. Med. 214 (2017) 2387–2404.
[53] R.L. Watson, W.Y. Lung, S.J. Bensinger, J.A. Belperio, Oropharyngeal administration of bleomycin in the murine model of pulmonary fibrosis, J. Vis. Exp. (2025) e67953, https://doi.org/10.3791/67953.
[54] B. Strobel, et al., Time and phenotype-dependent transcriptome analysis in AAV-TGFβ1 and Bleomycin-induced lung fibrosis models, Sci. Rep. 12 (2022) 12190.
[55] G. Izbicki, M.j. Segel, T.g. Christensen, M.w. Conner, R. Breuer, Time course of bleomycin-induced lung fibrosis, Int. J. Exp. Pathol. 83 (2002) 111–119.
[56] P. Kolb, et al., The importance of interventional timing in the bleomycin model of pulmonary fibrosis, Eur. Respir. J. 55 (2020).
[57] R.G. Jenkins, et al., An official American thoracic society workshop report: use of animal models for the preclinical assessment of potential therapies for pulmonary fibrosis, Am. J. Respir. Cell Mol. Biol. 56 (2017) 667–679.

[58] L.G. Bracaglia, et al., High-throughput quantitative microscopy-based half-life measurements of intravenously injected agents, Proc. Natl. Acad. Sci. 117 (2020) 3502–3508.
[59] I.V. Zelepukin, et al., Fast processes of nanoparticle blood clearance: comprehensive study, J. Contr. Release 326 (2020) 181–191.
[60] C. Marques, et al., Identification of the proteins determining the blood circulation time of nanoparticles, ACS Nano 17 (2023) 12458–12470.
[61] T. Yamamoto, et al., Pulmonary ventilation imaging based on 4-Dimensional computed tomography: Comparison with pulmonary function tests and SPECT ventilation images, Int. J. Radiat. Oncol. 90 (2014) 414–422.
[62] M.I. Love, W. Huber, S. Anders, Moderated estimation of fold change and dispersion for RNA-seq data with DESeq2, Genome Biol. 15 (2014) 1–21.
[63] N. Ignatiadis, B. Klaus, J.B. Zaugg, W. Huber, Data-driven hypothesis weighting increases detection power in genome-scale multiple testing, Nat. Methods 13 (2016) 577–580.
[64] A. Azuma, et al., Interferon-β inhibits bleomycin-induced lung fibrosis by decreasing transforming growth Factor-β and thrombospondin, Am. J. Respir. Cell Mol. Biol. 32 (2005) 93–98.
[65] T.R. Luckhardt, et al., TLR9-induced interferon β is associated with protection from gammaherpesvirus-induced exacerbation of lung fibrosis, Fibrogenesis Tissue Repair 4 (2011) 18.
[66] M.D. Wilkerson, D.N. Hayes, ConsensusClusterPlus: a class discovery tool with confidence assessments and item tracking, Bioinformatics 26 (2010) 1572–1573.
[67] L. Meyaard, et al., LAIR-1, a novel inhibitory receptor expressed on human mononuclear leukocytes, Immunity 7 (1997) 283–290.
[68] D. Pei, Leukolysin/MMP25/MT6-MMP: a novel matrix metalloproteinase specifically expressed in the leukocyte lineage, Cell Res. 9 (1999) 291–303.
[69] J.A. Ackermann, K. Hofheinz, M.M. Zaiss, G. Krönke, The double-edged role of 12/15-lipoxygenase during inflammation and immunity, Biochim. Biophys. Acta BBA - Mol. Cell Biol. Lipids 1862 (2017) 371–381.
[70] W.X. Zhang, P. Kubes, NOX2: is the best defense a good offense? Blood 139 (2022) 2851–2853.
[71] L. Swanson, et al., TLR4 signaling and macrophage inflammatory responses are dampened by GIV/girdin, Proc. Natl. Acad. Sci. 117 (2020) 26895–26906.
[72] Y. Cyr, et al., The IRG1–itaconate axis protects from cholesterol-induced inflammation and atherosclerosis, Proc. Natl. Acad. Sci. 121 (2024) e2400675121.
[73] J. Ji, et al., IRG1/ACOD1 promotes neutrophil reverse migration and alleviates local inflammation, J. Leukoc. Biol. 116 (2024) 854–863.
[74] M.F. Beers, E.E. Morrisey, The three r's of lung health and disease: repair, remodeling, and regeneration, J. Clin. Investig. 121 (2011) 2065–2073.
[75] J. Bhattacharya, M.A. Matthay, Regulation and repair of the alveolar-capillary barrier in acute lung injury, Annu. Rev. Physiol. 75 (2013) 593–615.
[76] A.L. McCubbrey, et al., Deletion of c-FLIP from CD11bhi macrophages prevents development of bleomycin-induced lung fibrosis, Am. J. Respir. Cell Mol. Biol. 58 (2018) 66–78.
[77] A.V. Misharin, L. Morales-Nebreda, G.M. Mutlu, G.R.S. Budinger, H. Perlman, Flow cytometric analysis of macrophages and dendritic cell subsets in the mouse lung, Am. J. Respir. Cell Mol. Biol. 49 (2013) 503–510.
[78] B. Becher, et al., High-dimensional analysis of the murine myeloid cell system, Nat. Immunol. 15 (2014) 1181–1189.
[79] M. Lech, H.-J. Anders, Macrophages and fibrosis: how resident and infiltrating mononuclear phagocytes orchestrate all phases of tissue injury and repair, Biochim. Biophys. Acta BBA - Mol. Basis Dis. 1832 (2013) 989–997.
[80] B.B. Moore, et al., Protection from pulmonary fibrosis in the absence of CCR2 signaling, J. Immunol. Baltim. Md 1950 167 (2001) 4368–4377.
[81] K.L. Wong, et al., Gene expression profiling reveals the defining features of the classical, intermediate, and nonclassical human monocyte subsets, Blood 118 (2011) e16–e31.
[82] P.B. Narasimhan, P. Marcovecchio, A.A.J. Hamers, C.C. Hedrick, Nonclassical monocytes in health and disease, Annu. Rev. Immunol. 37 (2019) 439–456.
[83] P. Ramachandran, et al., Differential Ly-6C expression identifies the recruited macrophage phenotype, which orchestrates the regression of murine liver fibrosis, Proc. Natl. Acad. Sci. 109 (2012) E3186–E3195.
[84] C. Mitchell, et al., Dual role of CCR2 in the constitution and the resolution of liver fibrosis in mice, Am. J. Pathol. 174 (2009) 1766–1775.
[85] K.R. Karlmark, et al., The fractalkine receptor CX3CR1 protects against liver fibrosis by controlling differentiation and survival of infiltrating hepatic monocytes, Hepatology 52 (2010) 1769–1782.
[86] E.L. Gautier, et al., Systemic analysis of PPARγ in mouse macrophage populations reveals marked diversity in expression with critical roles in resolution of inflammation and airway immunity, J. Immunol. 189 (2012) 2614–2624.
[87] S. Schif-Zuck, et al., Saturated-efferocytosis generates pro-resolving CD11blow macrophages: modulation by resolvins and glucocorticoids, Eur. J. Immunol. 41 (2011) 366–379.
[88] S. Butenko, et al., Transcriptomic analysis of monocyte-derived non-phagocytic macrophages favors a role in limiting tissue repair and fibrosis, Front. Immunol. 11 (2020).
[89] J.R. Podojil, et al., Biodegradable nanoparticles induce cGAS/STING-dependent reprogramming of myeloid cells to promote tumor immunotherapy, Front. Immunol. 13 (2022).
[90] J.R. Shaw, et al., Inflammatory disease progression shapes nanoparticle biomolecular corona-mediated immune activation profiles, Nat. Commun. 16 (2025) 924.
[91] D.M. Underhill, H.S. Goodridge, Information processing during phagocytosis, Nat. Rev. Immunol. 12 (2012) 492–502.
[92] J.M. Ratter, et al., In vitro and in vivo effects of lactate on metabolism and cytokine production of human primary PBMCs and monocytes, Front. Immunol. 9 (2018).
[93] H. Cai, et al., Lactate activates trained immunity by fueling the tricarboxylic acid cycle and regulating histone lactylation, Nat. Commun. 16 (2025) 3230.
[94] C.V. Maduka, et al., Immunometabolic cues recompose and reprogram the microenvironment around implanted biomaterials, Nat. Biomed. Eng. 8 (2024) 1308–1321.
[95] C.Y. Perrot, T. Karampitsakos, J.D. Herazo-Maya, Monocytes and macrophages: emerging mechanisms and novel therapeutic targets in pulmonary fibrosis, Am. J. Physiol. Cell Physiol. 325 (2023) C1046–C1057.
[96] K. Kawamura, et al., Monocyte count and the risk for acute exacerbation of fibrosing interstitial lung disease: a retrospective cohort study, Chron. Respir. Dis. 17 (2020) 1479973120909840.
[97] C. Guo, et al., Single-cell analysis of two severe COVID-19 patients reveals a monocyte-associated and tocilizumab-responding cytokine storm, Nat. Commun. 11 (2020) 3924.
[98] N.I. Popescu, C. Lupu, F. Lupu, Disseminated intravascular coagulation and its immune mechanisms, Blood 139 (2022) 1973–1986.
[99] A. Takala, et al., A prospective study of inflammation markers in patients at risk of indirect acute lung injury, Shock 17 (2002) 252.
[100] T. Zaman, et al., Differences in clinical characteristics and outcomes between men and women with idiopathic pulmonary fibrosis: a multicenter retrospective cohort study, Chest 158 (2020) 245–251.
[101] N. Caporarello, et al., Vascular dysfunction in aged mice contributes to persistent lung fibrosis, Aging Cell 19 (2020) e13196.